Modified Look-Locker Inversion Recovery (MOLLI) for High-Resolution T_1 Mapping of the Heart

Daniel R. Messroghli,[1*] Aleksandra Radjenovic,[2] Sebastian Kozerke,[3] David M. Higgins,[4] Mohan U. Sivananthan,[1] and John P. Ridgway[4]

A novel pulse sequence scheme is presented that allows the measurement and mapping of myocardial T_1 in vivo on a 1.5 Tesla MR system within a single breath-hold. Two major modifications of conventional Look-Locker (LL) imaging are introduced: 1) selective data acquisition, and 2) merging of data from multiple LL experiments into one data set. Each modified LL inversion recovery (MOLLI) study consisted of three successive LL inversion recovery (IR) experiments with different inversion times. We acquired images in late diastole using a single-shot steady-state free-precession (SSFP) technique, combined with sensitivity encoding to achieve a data acquisition window of <200 ms duration. We calculated T_1 using signal intensities from regions of interest and pixel by pixel. T_1 accuracy at different heart rates derived from simulated ECG signals was tested in phantoms. T_1 estimates showed small systematic error for T_1 values from 191 to 1196 ms. In vivo T_1 mapping was performed in two healthy volunteers and in one patient with acute myocardial infarction before and after administration of Gd-DTPA. T_1 values for myocardium and noncardiac structures were in good agreement with values available from the literature. The region of infarction was clearly visualized. MOLLI provides high-resolution T_1 maps of human myocardium in native and post-contrast situations within a single breath-hold. Magn Reson Med 52:141–146, 2004. © 2004 Wiley-Liss, Inc.

Key words: spin-lattice relaxation time; Look-Locker; heart; myocardium

Despite recent technological advances, in vivo T_1 quantification of the myocardium with modern magnetic resonance (MR) systems remains a challenge because of severe time constraints due to cardiac and respiratory motion. While myocardial T_1 is shorter and therefore relatively easier to measure at low field strengths, it has a value of ~1000 ms at a field strength of 1.5 T, exceeding the duration of the cardiac cycle (~600–1200 ms) in most subjects (1,2). Since standard inversion recovery (IR) measurements require a relaxation period of four to five times T_1 to allow for full magnetization recovery after each 180° pulse (3), only four to five such single-point IR experiments can be performed within one breath-hold (ca. 20 s). To achieve accurate T_1 estimates from a three-parameter curve-fitting

procedure, as is commonly employed, data from at least six to 10 time points should be available (4). The multipoint approach, as first described by Look and Locker (5), samples the relaxation curve multiple times after an initial preparation pulse (6). This technique has been shown theoretically to be highly efficient (7), and has been widely used for T_1 measurements of the brain (8–11). It is not suitable for pixel-by-pixel T_1 mapping of the heart because data acquisition is performed continuously throughout the cardiac cycle without regard for cardiac motion, which means that T_1 values can only be derived for regions of interest (ROIs) that must be defined manually for every frame (1). The resultant T_1 values may consequently be subject to inaccuracy caused by misregistration effects.

In this work we present a pulse sequence scheme that allows for accurate in vivo T_1 measurements and T_1 mapping of myocardium with high spatial resolution and within a single breath-hold. To overcome the limitations of the conventional LL approach for cardiac applications, we propose a modified LL IR scheme (MOLLI), which introduces two principles to the standard LL sequence: 1) selective data acquisition at a given time of the cardiac cycle over successive heartbeats, and (2) merging of image sets from multiple LL experiments with varying inversion times (TIs) into one data set. While selective data acquisition effectively decreases the number of images acquired in each LL experiment to one per heartbeat, the use of multiple LL experiments with different TIs increases the number of samples of the relaxation curve to a value that is sufficiently high for accurate T_1 estimation. The IR preparation pulse is used to yield the maximum dynamic range of the signal. A balanced steady-state free precession (SSFP) readout is chosen over conventional gradient-echo (GE) readout because of its higher signal-to-noise ratio (SNR) and lower tendency to modulate the relaxation curve (12). To minimize artifacts from cardiac motion, the image data acquisition window is restricted to <200 ms in end-diastole by the use of sensitivity encoding (SENSE) (13) with a reduction factor of 2. We investigated the accuracy of T_1 measurements with MOLLI using gel phantoms for a wide range of heart rates derived from simulated electrocardiogram (ECG) signals. T_1 maps and the T_1 values derived from in vivo experiments in two healthy volunteers and one patient with acute myocardial infarction are presented.

MATERIALS AND METHODS

Pulse Sequence Scheme

The MOLLI pulse sequence scheme is illustrated in Fig. 1. Three successive ECG-triggered LL experiments (LL$_1$, LL$_2$, and LL$_3$) were carried out with three, three, and five single-shot readouts, respectively. Undisturbed magnetization recovery was allowed for at least 4 s between each LL ex-

[1]BHF Cardiac MRI Unit, Leeds General Infirmary, Leeds, UK.

[2]Academic Unit of Medical Physics, University of Leeds, Leeds, UK.

[3]Institute for Biomedical Engineering, ETH and University of Zurich, Zurich, Switzerland.

[4]Department of Medical Physics, Leeds General Infirmary, Leeds, UK.

*Correspondence to: Dr. Daniel Messroghli, BHF Cardiac MRI Unit, Leeds General Infirmary, B-Floor, Clarendon Wing, Great George Street, Leeds LS1 3EX, UK. E-mail: daniel@messroghli.de
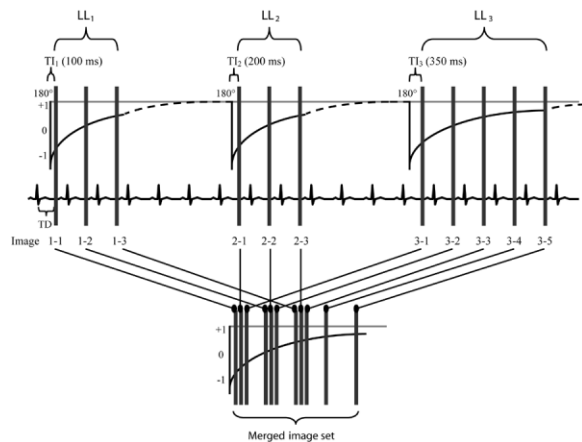
FIG. 1. MOLLI pulse sequence scheme. Vertical bars represent image acquisition. Dashed lines represent undisturbed signal recovery. Three sets of LL experiments were performed successively with increasing TI within one breath-hold's time. Images were acquired with a specific trigger delay (TD) to select end-diastole. For post-processing (calculation of T_1 values), the images were regrouped into one data set according to their effective TI.

periment, with variation dependent on the subjects' heart rate, and the reconstruction and preparation time of the MR scanner. In each of the three LL experiments, the first single-shot readout was performed at TI ($LL_1 = 100$ ms, $LL_2 = 200$ ms, and $LL_3 = 350$ ms) after a non-slice-selective adiabatic 180° pulse and at delay time TD after the previous R-wave. Subsequent images were acquired at time TD after every R-wave, until the final number of images for each LL experiment was acquired. Data acquisition consisted of a single-slice, single-shot, balanced SSFP pulse sequence (balanced turbo-field echo (BTFE)) combined with SENSE with a reduction factor of 2, number of lines of k-space (TFE factor) = 49, dummy acquisitions = 13, partial Fourier acquisition, flip angle = 50°, repetition time (TR) = 3.9 ms, echo time (TE) = 1.95 ms, field of view (FOV) = 380 × 342 mm, matrix = 240 × 151, measured pixel size = 1.58 × 2.26 mm, slice thickness = 8 mm, and acquisition window = 191.1 ms.

Phantom Studies

The MR studies were performed on a 1.5 T Gyroscan Intera CV MR system (Philips, Best, The Netherlands) with Master gradients (30 mT/m, 150 T/m/s). Seven agarose gel phantoms doped with different amounts of gadolinium-EDTA were studied. After a SENSE reference scan was acquired, two series of MOLLI experiments were performed with a five-element cardiac phased-array coil at "heart rates" of 40–100 beats per min (bpm), which were derived from user-defined

simulated ECG signals. The first of these two sets was performed in ascending order, and the second set was performed in descending order of heart rate. Reference values of T_1 were established following the MOLLI experiments by means of a standard multipoint IR spin-echo technique (TI = 50–10000 ms) with a birdcage head coil.

T_1 Calculations

Images were sorted according to their accumulative time from inversion (t), which is given by

$$t = TI + (n - 1)RR, \qquad [1]$$

where N = image number within the LL experiment, and RR = heartbeat interval. Three-parameter nonlinear curve fitting (14) using a Levenberg-Marquardt algorithm was performed for

$$y = A - B \exp(- t/T_1^*), \qquad [2]$$

for corresponding ROIs (Origin 7; OriginLab Corp., Northampton, MA) and for corresponding pixels (customized T_1 mapping software written in IDL 6.0; RSI UK Ltd., Berkshire, UK). In Eq. [2], y denotes signal intensity, and T_1^* corresponds to the apparent, modified T_1 in an LL experiment. We assigned signal polarity for the magnitude images using the approach described by Nekolla et al. (15). This involves the creation of multiple data sets: the first set has all points on the curve assigned as positive values, the second set has the first point of the curve assigned as negative, the third set has the first two points of the curve assigned as negative, and so on. From these sets, the one with the best quality of fit, as defined by the lowest value of chi-square, is selected.

T_1 was calculated from the resulting parameters T_1^*, A, and B by applying the equation

$$T_1 = T_1^*((B/A) - 1), \qquad [3]$$

as used for studies with conventional LL techniques (16).

To calculate the standard deviation (SD) of the combined estimation error of T_1, we added the errors of the three fitting parameters in quadrature.

In Vivo Studies

The study was approved by the local ethics committee, and written informed consent was obtained from all of the subjects. In vivo experiments were performed in the same manner as the phantom studies in two healthy volunteers in mid-cavity short-axis slices before and 10 min after intravenous application of 0.15 mmol/kg gadolinium-DTPA (Magnevist; Schering AG, Berlin, Germany). All of

Table 1
Subject Characteristics

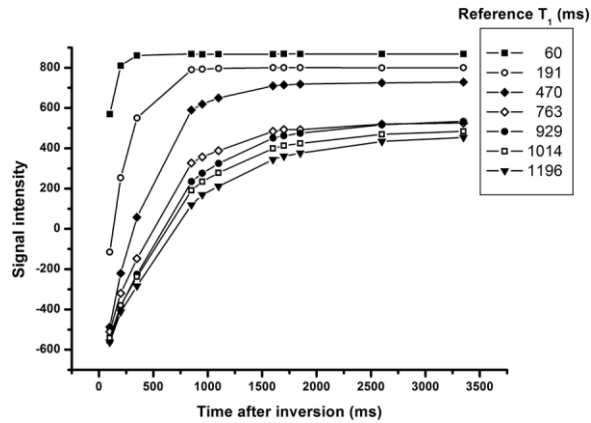|	Age (y)	Sex	Height (cm)	Weight (kg)	Heart rate (bpm)
Volunteer 1	33	Male	190	94	80
Volunteer 2	35	Female	165	63	75
Patient	52	Male	179	90	70

FIG. 2. Signal intensity curves (with restored signs) for the seven gel phantoms at a simulated heart rate of 80 bpm. With very short T_1 (60 ms), a signal plateau is already reached at the third sample point.

FIG. 3. Percentage error in T_1 estimation at different simulated heart rates as compared to reference values.

the MOLLI studies were performed in single breath-holds. One patient with acute anteroseptal myocardial infarction (day 5, peak creatine kinase = 613 U/l, nonreperfused) underwent the same protocol (except for FOV = 410 × 369 mm, and pixel size = 1.71 × 2.44 mm) plus subsequent conventional delayed-enhancement imaging in the same slice (IR-prepared GE, TR = 4.5 ms, TE = 1.8 ms, TI = 260 ms, and the same geometric parameters as for the MOLLI images). Details regarding the subjects are given in Table 1. Quantitative T_1 maps were calculated in the same manner as for the phantom studies except that instead of using Eq. [1], we extracted the accumulative time from inversion directly from the headers of the images' DICOM files as recorded by the MR system. Mean T_1 values were obtained for ROIs placed on the T_1 maps in normal myocardium, infarcted myocardium (in the patient with myocardial infarction), left ventricular (LV) blood pool, skeletal muscle, and liver with the use of a commercial software package (Mass 5.0; Medis, Leiden, The Netherlands).

RESULTS

Phantom Studies

Figure 2 gives signal intensity curves (with restored signs) for the seven gel phantoms at a simulated heart rate of 80 bpm. Table 2 gives the reference values for T_1 of the gel
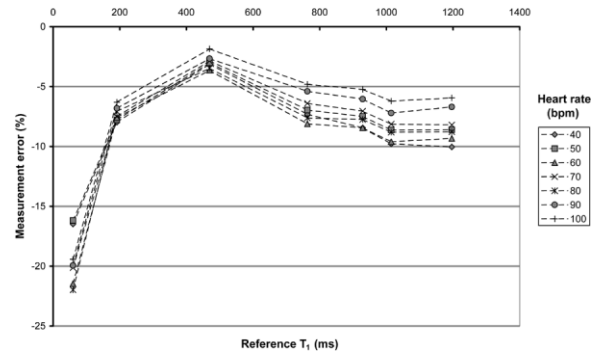
phantoms, as well as the results for the first series of MOLLI studies at heart rates of 40–100 bpm. Figure 3 shows the percentage error in T_1 estimation at different heart rates as compared to reference values. The duration of the breath-hold MOLLI data acquisitions ranged from 14.7 to 23 s. There was a systematic underestimation of T_1, with maximum error of −10.0% (mean ± SD: −6.8 ± 2.1%) for T_1 values from 191 to 1196 ms, and with maximum error of −22% for T_1 = 60 ms. Underestimation was more pronounced for lower heart rates and for very high or very low values of T_1. Series 2 (varying of heart rate in descending order; results not shown) produced the same pattern of measurement error as series 1, confirming the initial results (maximum error of series 2: −10.1%, mean ± SD: −5.8 ± 2.9%, Pearson's correlation for T_1 values of series 1 vs. series 2: r = 0.999, $P < 0.001$, N = 49).

In Vivo Studies

Pre- and postcontrast T_1 maps are shown in Fig. 4 for the two volunteers, and in Fig. 5 for the patient with acute myocardial infarction. The duration of the MOLLI studies ranged from 15.1 to 18.2 s. There was a clear delineation of the LV wall and the papillary muscles in all three cases. Table 3 summarizes the T_1 values (± SD) derived from ROIs for different tissues. T_1 values for the myocardium, LV blood pool, skeletal muscle, and liver were in good agreement with corresponding values available from the literature (1,2,17,18). In the patient, the area of infarction showed a markedly increased T_1 value as compared to

Table 2

T_1 Values (ms) ±SD Measured in a Set of MOLLI Experiments in Phantoms With Different Reference T_1 at Simulated Heart Rates From 40 to 100 bpm

Heart rate (bpm)	Reference T_1 (ms)						
	60	191	470	763	929	1014	1196
40	50 ± 0.6	176 ± 0.8	455 ± 4.3	707 ± 8.8	850 ± 8.6	915 ± 9.6	1076 ± 10.1
50	50 ± 0.6	176 ± 0.8	455 ± 5.5	710 ± 10.1	859 ± 10.3	927 ± 11.3	1093 ± 12.8
60	47 ± 0.8	177 ± 1.1	452 ± 5.8	701 ± 10.2	850 ± 10.3	917 ± 11.4	1085 ± 12.4
70	48 ± 0.6	177 ± 1.3	456 ± 6.6	714 ± 11.5	863 ± 12.0	932 ± 13.5	1098 ± 15.2
80	47 ± 0.7	178 ± 1.5	453 ± 6.4	705 ± 11.3	857 ± 11.6	925 ± 13.0	1091 ± 15.0
90	48 ± 0.7	178 ± 1.7	457 ± 6.9	722 ± 12.1	873 ± 12.7	941 ± 14.7	1116 ± 17.4
100	48 ± 0.6	179 ± 1.9	461 ± 7.3	726 ± 13.4	880 ± 14.3	951 ± 16.7	1125 ± 20.1
Mean	48.1 ± 1.3	177.4 ± 1.1	455.7 ± 2.8	712.2 ± 9.1	861.9 ± 11.2	929.7 ± 13.0	1097.8 ± 17.3

Native   **10 min post-CM**
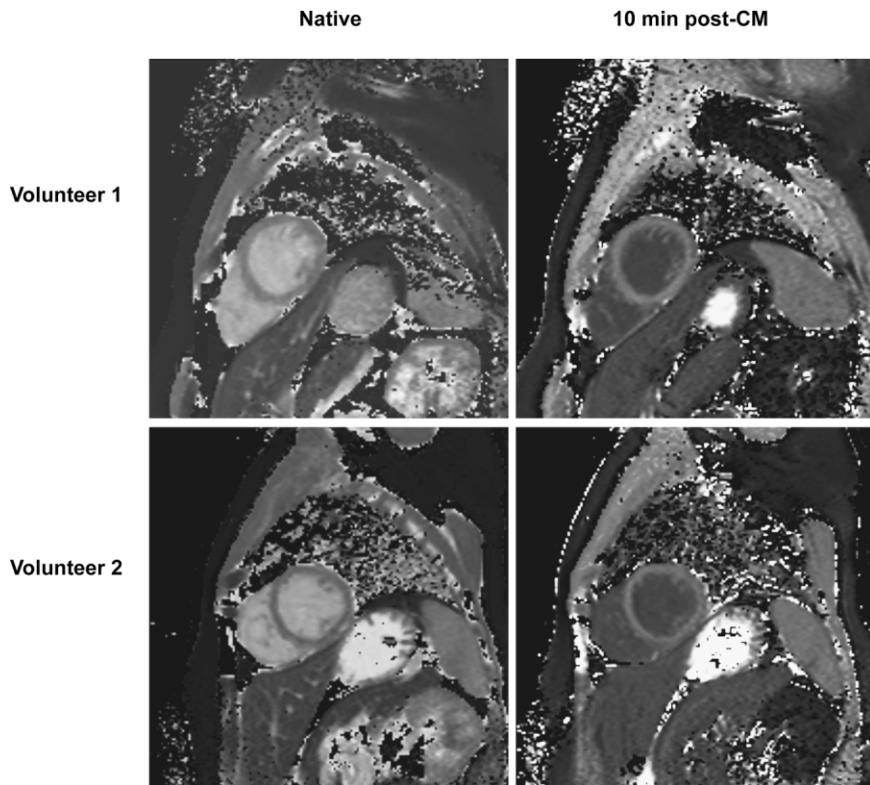
Volunteer 1

FIG. 4. Pre- and postcontrast mid-cavity short-axis T_1 maps of two healthy volunteers.

Volunteer 2

remote myocardium (1360 ± 104 vs. 948 ± 67 ms, respectively) except for the subendocardial region at the center (1106 ± 72 ms). After the application of contrast medium, T_1 in the outer layer of the infarcted area was 37.4% lower than T_1 in remote myocardium (281 ± 44 vs. 449 ± 35 ms), corresponding to prolonged wash-out of contrast medium in the necrotic area that was visualized as "delayed enhancement" in the IR-prepared GE image. The center of the infarcted area exhibited a T_1 relaxation time that was higher than that of remote myocardium (511 ± 114 vs. 449 ± 35 ms, respectively) and presented as a "hypoenhanced core" on the IR-prepared GE image.

DISCUSSION

The MOLLI imaging scheme achieved highly accurate T_1 measurements in phantoms of various T_1 times, covering the full range of T_1 that can be expected in human soft tissues under both native and contrast medium-enhanced conditions. The size of the observed measurement error was comparable to that seen in conventional fast T_1 measurement techniques used for brain studies (9–11).

Compared to the T_1 mapping technique described by Wacker et al. (2,19) in a study using multishot saturation recovery images, MOLLI images have a higher matrix (240 × 151 vs. 128 × 80) despite their lower acquisition time (191 vs. 230 ms), and hold higher dynamic signal range due to the use of an inversion pulse instead of a saturation pulse. This explains the good results of the in vivo part of this study, in which quantitative T_1 maps of mid-ventricular short-axis slices were obtained within single breath-holds in volunteers and in a patient with acute myocardial infarction. The image quality of the T_1 maps was high enough for relatively small anatomical structures, such as papillary muscles within the heart or veins in the liver, to be identified.
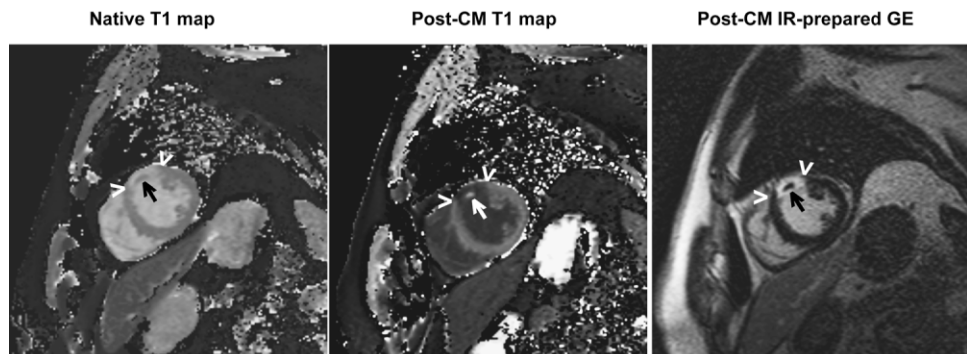
Native T1 map   **Post-CM T1 map**   **Post-CM IR-prepared GE**

FIG. 5. Pre- and post-contrast short-axis T_1 maps and corresponding conventional IR-prepared GE image with "delayed enhancement" in a patient with acute anteroseptal myocardial infarction (extent of infarct-related signal changes marked by arrowheads; arrow indicates the "hypoenhanced core" phenomenon).

Table 3
T_1 Values (ms) Obtained From MOLLI T_1 Maps Before (Native) and After Administration of Contrast Medium (CM), Derived From Regions-of-Interest for Normal Myocardium, Skeletal Muscle, Liver, and Left Ventricular Blood Pool

	Myocardium		Skeletal muscle		Liver		Blood	
	Native	CM	Native	CM	Native	CM	Native	CM
Volunteer 1	1076 ± 72	492 ± 39	794 ± 109	535 ± 47	666 ± 64	347 ± 18	1551 ± 55	313 ± 10
Volunteer 2	969 ± 84	450 ± 40	769 ± 35	475 ± 18	611 ± 23	333 ± 19	1544 ± 69	325 ± 14
Patient	948 ± 67	449 ± 35	719 ± 68	510 ± 40	591 ± 63	304 ± 26	1518 ± 69	266 ± 14

The T_1 values derived for normal myocardium and various noncardiac tissues compared favorably to those reported in the literature for measurements at 1.5 T (1,2,17,18). In agreement with reports from low-field systems (20) and from a preliminary high-field study (21), the area of infarction in our patient was visualized on native images as a region of increased T_1 times. After the contrast medium was applied, the infarcted region presented as a region with markedly lower T_1 times compared to the remote myocardium, corresponding to the "delayed enhancement" phenomenon commonly utilized for viability imaging (22,23). Pre- and postcontrast T_1 maps also clearly visualized the subendocardial "hypoenhanced core" phenomenon (24) observed in this patient on the conventional IR-prepared GE image. To our knowledge, this is the first time that absolute measurements of pre- and postcontrast T_1 values have been derived for such regions directly from a parametric image. This presents a new perspective for the analysis of delayed enhancement, which heretofore (with the use of IR-prepared GE pulse sequences) could only be quantified in terms of its spatial extent, whereas the degree of signal changes as compared to normal myocardium could only be differentiated as "present" or "not present."

The heart-rate dependency of the measurement error seen in the phantoms can be attributed to the differences in the delay times of the LL readouts caused by different heartbeat intervals at different heart rates, which in turn lead to differences in the recovery behavior of the relaxation curve. As shown by Scheffler et al. (12), balanced SSFP pulse sequences (as used for this study) in general introduce only a little perturbation of the relaxation curve compared to conventional fast GE pulse sequences, such as fast low-angle shot (Turbo-FLASH). This explains why T_1 values in the range of 191–1196 ms in our study differed by a maximum of only 4.1% when the heart rate was varied between 40 and 100 bpm. The effect of the perturbation induced by the acquisition is that the relaxation curve reaches an asymptotic value more rapidly, which may explain the finding that T_1 was systematically underestimated.

With the given choice of image parameters, the same accuracy as for the range of 191–1196 ms could not be reached for very low T_1 values (60 ms), since there were not enough very early sampling points for the curve-fitting procedure, as illustrated by Fig. 2. To achieve higher accuracy in this low T_1 range, a different timing scheme (with additional LL experiments or earlier initial TI of the third LL experiment) would have to be used. However, in human myocardium, T_1 values of <200 ms are not expected when clinical doses of contrast medium are used.

The agreement of the results from series with ascending and descending heart-rate orders rules out radiofrequency power-induced thermal changes within the phantoms as a cause of the observed heart-rate dependency. Because of its systematic nature, the measurement error could in principle be corrected for mathematically; however, the investigation of such a correction is beyond the scope and design of this study. It could be postulated that a correction for heart rate may increase the reproducibility of myocardial T_1 measurements in the general population. Further investigations with a larger number of subjects will be necessary to answer this question.

CONCLUSIONS

With the use of the MOLLI imaging scheme, highly accurate measurements of a wide range of T_1 were performed in vitro. High-resolution T_1 maps were acquired in vivo, both before and after the application of contrast medium, yielding T_1 values for a number of different tissues, including myocardium, which agree well with those found in the literature. Signal changes in areas with delayed enhancement were quantified. MOLLI provides a promising tool for the measurement of myocardial T_1 times under clinical conditions.

ACKNOWLEDGMENTS

REFERENCES

1. Flacke SJ, Fischer SE, Lorenz CH. Measurement of the gadopentetate dimeglumine partition coefficient in human myocardium in vivo: normal distribution and elevation in acute and chronic infarction. Radiology 2001;218:703–710.
2. Wacker CM, Bock M, Hartlep AW, Beck G, Van Kaick, Ertl G, Bauer WR, Schrad LR. Changes in myocardial oxygenation and perfusion under pharmacological stress with dipyridamole: assessment using T*2 and T1 measurements. Magn Reson Med 1999;41:686–695.
3. Pykett IL, Rosen BR, Buonanno FS, Brady TJ. Measurement of spin-lattice relaxation times in nuclear magnetic resonance imaging. Phys Med Biol 1983;28:723–729.
4. Zhang Y, Yeung HN, O'Donnell M, Carson PL. Determination of sample time for T1 measurement. J Magn Reson Imaging 1998;8:675–681.
5. Look DC, Locker DR. Time saving in measurement of NMR and EPR relaxation times. Rev Sci Instrum 1970;41:250–251.

6. Graumann R, Barfuβ H, Hentschel D, Oppelt A. TOMROP: eine Sequenz zur Bestimmung der Längsrelaxationszeit T1 in der Kernspintomographie. Electromedica 1987;55:67–72.

7. Crawley AP, Henkelman RM. A comparison of one-shot and recovery methods in T1 imaging. Magn Reson Med 1988;7:23–34.

8. Brix G, Schad LR, Deimling M, Lorenz WJ. Fast and precise T_1 imaging using a TOMROP sequence. Magn Reson Imaging 1990;8:351–356.

9. Freeman AJ, Gowland PA, Mansfield P. Optimization of the ultrafast Look-Locker echo-planar imaging T1 mapping sequence. Magn Reson Imaging 1998;16:765–772.

10. Henderson E, McKinnon G, Lee TY, Rutt BK. A fast 3D Look-Locker method for volumetric T1 mapping. Magn Reson Imaging 1999;17:1163–1171.

11. Karlsson M, Nordell B. Phantom and in vivo study of the Look-Locher T1 mapping method. Magn Reson Imaging 1999;17:1481–1488.

12. Scheffler K, Hennig J. T(1) quantification with inversion recovery TrueFISP. Magn Reson Med 2001;45:720–723.

13. Pruessmann KP, Weiger M, Scheidegger MB, Boesiger P. SENSE: sensitivity encoding for fast MRI. Magn Reson Med 1999;42:952–962.

14. Sass M, Ziessow D. Error analysis for optimized inversion recovery spin-lattice relaxation measurements. J Magn Reson 1977;25:263–276.

15. Nekolla S, Gneiting T, Syha J, Deichmann R, Haase A. T1 maps by k-space reduced snapshot-FLASH MRI. J Comput Assist Tomogr 1992; 16:327–332.

16. Deichmann R, Haase A. Quantification of T1 values by snapshot-FLASH NMR imaging. J Magn Reson 1992;96:608–612.

17. Wagenseil JE, Johansson LO, Lorenz CH. Characterization of T1 relaxation and blood-myocardial contrast enhancement of NC100150 injection in cardiac MRI. J Magn Reson Imaging 1999;10:784–789.

18. Bottomley PA, Foster TH, Argersinger RE, Pfeifer LM. A review of normal tissue hydrogen NMR relaxation times and relaxation mechanisms from 1–100 MHz: dependence on tissue type, NMR frequency, temperature, species, excision, and age. Med Phys 1984;11: 425–448.

19. Wacker CM, Fidler F, Dueren C, Hirn S, Jakob PM, Ertl G, Haase A, Bauer WR. Quantitative assessment of myocardial perfusion with a spin-labeling technique: preliminary results in patients with coronary artery disease. J Magn Reson Imaging 2003;18:555–560.

20. Been M, Smith MA, Ridgeway JP, Brydon JW, Douglas RH, Kean DM, Best JJ, Muir AL. Characterisation of acute myocardial infarction by gated magnetic resonance imaging. Lancet 1985;2:348–350.

21. Messroghli DR, Niendorf T, Schulz-Menger J, Dietz R, Friedrich MG. T1 mapping in patients with acute myocardial infarction. J Cardiovasc Magn Reson 2003;5:353–359.

22. Simonetti OP, Kim RJ, Fieno DS, Hillenbrand HB, Wu E, Bundy JM, Finn JP, Judd RM. An improved MR imaging technique for the visualization of myocardial infarction. Radiology 2001;218:215–223.

23. Kim RJ, Fieno DS, Parrish TB, Harris K, Chen EL, Simoneth O, Bundy J, Finn JP, Klocke FJ, Judd RM. Relationship of MRI delayed contrast enhancement to irreversible injury, infarct age, and contractile function. Circulation 1999;100:1992–2002.

24. Wu KC, Zerhouni EA, Judd RM, Lugo-Olivieri CH, Barouch LA, Schulman SP, Blumenthal RS, Lima JA. Prognostic significance of microvascular obstruction by magnetic resonance imaging in patients with acute myocardial infarction. Circulation 1998;97:765–772.